Structural and morphological control of nano-sized Cu islands on SiO_2 using a Ti underlayer

Minghui Hu,[a] Suguru Noda,[b] Tatsuya Okubo, Yukio Yamaguchi, and Hiroshi Komiyama

Department of Chemical System Engineering, University of Tokyo

7-3-1 Hongo, Bunkyo-ku, Tokyo 113-8656, Japan

Abstract

The structure and morphology of nano-sized Cu islands grown by sputter deposition on SiO_2 substrates without and with a 5-nm Ti underlayer are investigated using transmission electron microscopy. On SiO_2, spherical Cu islands with a random crystalline orientation are formed, whereas on Ti/SiO_2, semi-spherical islands with a preferred <111> crystalline orientation are formed. Moreover, the Cu islands on Ti/SiO_2 have a larger size, longer inter-island distance, and higher number density than those on SiO_2. These structural and morphological changes at the nanoscale are discussed from

[a] Authors to whom correspondence should be addressed; electronic mail: mhu@chemsys.t.u-tokyo.ac.jp

[b] Also could be addressed to; electronic mail: noda@chemsys.t.u-tokyo.ac.jp

the viewpoint of interfacial interactions. Our study suggests that by using an appropriate metal underlayer, it is possible to fabricate nano-sized islands with the desired wettability, crystalline orientation, as well as morphology of island ensembles.

I. INTRODUCTION

With the continuous scaledown of ultra-large-scale integrations (ULSI), and the rapid development of quantum devices with enhanced optic, electronic, and magnetic performances, the structural and morphological control of nano-sized three-dimensional (3D) islands formed during the initial stages of thin film growth is becoming increasingly significant. The wettability[1-3] and crystallographic structure[4-7] of nano-sized islands are determined by thermodynamic factors represented as surface/interface energies. On the other hand, the time-dependent morphology of island ensembles, such as island size, inter-island distance, and island number density,[8-11] is determined by kinetic factors represented as adatom/island mobility. Because both thermodynamic and kinetic factors are related to island/substrate interfacial interactions, nano-sized islands with the desired structure and morphology should be formed under controlled interfacial interactions. However, little has been reported about the attempt at the structural and morphological control of nano-sized islands, and its effects on the structure of continuous thin films.

The purpose of this study is to systematically investigate how the island wettability, crystalline orientation, and the morphology of island ensembles can be controlled using surface modification technologies. Cu/SiO_2, widely used in ULSI and catalysis, is selected as the study subject. We use Ti as an underlayer between Cu and SiO_2 to adjust the interfacial interactions, because on Ti substrates, Cu thin films have excellent adhesion,[12,13] and grow with an <111> texture.[14,15] In this paper, the initial growth of sputter deposited Cu on bare SiO_2 and SiO_2 with a Ti underlayer is investigated. The

differences in the wettability and crystalline orientation of nano-sized Cu islands, as well as their morphological evolution, are compared and discussed from the viewpoint of interfacial interactions.

II. EXPERIMENTAL

Si(100) wafers with a thermally oxidized, 10- to 15-nm SiO_2 layer were washed using an H_2SO_4/H_2O_2 solution. A radio-frequency magnetron sputter system equipped with Cu, Ti, and SiO_2 targets was used to deposit thin films onto substrates in a pure Ar atmosphere. The base pressure prior to deposition and the working pressure during the deposition were 4.0×10^{-5} and 0.8 Pa, respectively. Cu was deposited on SiO_2 substrates without and with a 5-6 nm Ti underlayer pre-grown in the same sputter chamber. To avoid structural variations during TEM specimen preparation and observation, a 10-nm SiO_2 cap layer was further deposited onto the Cu thin films. All of the depositions were conducted continuously without breaking the chamber vacuum. The deposition rate, R_f, of Cu and Ti was 0.11 nm/s, which was estimated by plotting the film thickness, h_f, versus the deposition time, t_d, after the formation of the continuous films. For Cu, this R_f equals approximately 0.5 monolayers/s or 9.1×10^{18} atoms/s·m^2, according to the lattice constant (0.21 nm) and the packing density (1.77×10^{19} Cu atoms/m^2) of the (111) planes of face-centered cubic (fcc) Cu.

Transmission electron microscopy (TEM) images and selected area electron diffraction (SAED) patterns were taken using a JEOL JEM2010F operating at 200 kV. The specimens for TEM observation were prepared using conventional mechanical

grinding, polishing, and dimpling, followed by Ar ion milling at an acceleration voltage of 4 keV and an incidence angle of 6°. X-ray diffraction (XRD) was used to investigate the texture of continuous Cu thin films. XRD patterns were recorded using Cu-Kα radiation in a RINT2400 (RIGAKU) operating at 40 kV and 200 mA.

III. RESULTS

A. Wettability of nano-sized Cu islands

The cross-sectional TEM (XTEM) images of Cu thin films on SiO_2 and Ti/SiO_2 at deposition times of t_d = 5 and 10 s are shown in Figs. 1 and 2, respectively. Although Cu grows in 3D mode on both of the substrates, these islands have different outer shapes. On SiO_2, the Cu islands appear completely spherical, and do not wet at all, whereas on Ti/SiO_2, the Cu islands appear semi-spherical, and partially wet. The high-resolution cross-sectional TEM (HRXTEM) images in Figs. 3 and 4 show more clearly the difference in wettability of the Cu islands on SiO_2 and Ti/SiO_2. In contrast to the wetting angle (θ) of 180° for the Cu islands on SiO_2, most of the Cu islands wet on Ti/SiO_2 with $\theta = 50 \pm 20°$.

Most studies on metal wettability on substrates are focused either on the liquid phase at high temperatures or at the submicron scale. Our experiment indicates that the nano-sized Cu islands show different wettabilities on different substrates. The wettability of these islands on SiO_2 can be controlled from non-wetting to wetting using Ti as an underlayer.

B. Crystalline orientation of nano-sized Cu islands

The HRXTEM images shown in Figs. 3 and 4 show the crystalline orientation of Cu islands on SiO_2 and Ti/SiO_2 at t_d = 5 and 10 s, respectively. As shown in Fig. 3, for the Cu islands on SiO_2, the Cu (111) planes have a vertical angle of 9.8°, 45.6°, 39.8°, and 85.0°, respectively. The difference between any two of them has a large deviation (>15°) from the standard dihedral angle of two (111) planes of Cu fcc structure (70.5°). Therefore, the Cu islands on SiO_2 appear randomly orientated. In contrast, for the Cu islands on Ti/SiO_2 [Fig. 4], Cu (111) planes are almost horizontal, and this orientation appears more precise at t_d = 10 s than at t_d = 5 s. Therefore, the Cu islands on Ti/SiO_2 are <111> orientated, and tend to develop with deposition time.

The plan-view TEM images and SAED patterns as shown in Fig. 5 support the above results from the HRXTEM images. For the Cu islands on SiO_2, the SAED patterns in Figs. 5(a) and 5(b) exhibit diffraction rings with the sequence of (111) > (200) > (220) in strength. Their strength from the Cu powder pattern is 100%, 46%, and 20%, respectively [Ref. JCPDS 4-0836]. The qualitative coincidence indicates that these Cu islands have a random crystalline orientation. However, for the Cu islands on Ti/SiO_2, the SAED patterns in Figs. 5(c) and 5(d) exhibit two facts. One is the absence of the (200) diffraction ring at t_d = 5 and 10 s. Another is the decreased strength for the (111) diffraction ring and the increased strength for the (220) diffraction ring at t_d = 10 s. These results also demonstrate that the Cu islands on Ti/SiO_2 are <111> orientated, and this preferential orientation develops with deposition time.

The crystallographic relation between the Cu islands and the Ti underlayer is analyzed as follows. As shown in the HRXTEM images in Fig. 4, the (0002) planes of the Ti hexagonal closest packing (hcp) structure are almost perpendicular to the thin film growth direction. Moreover, as shown in the plan-view SAED patterns in Figs. 5(c) and 5(d), only the (khl0) diffraction rings of the Ti hcp structure appear, and the (hkl1) diffraction ring is absent, which agrees with the presence of $(01\bar{1}0)$ lattice structure of hcp Ti shown in the plan-view high-resolution TEM (HRTEM) image [Fig. 6(a)]. Therefore, an identical conclusion is drawn from all of these results that the Ti underlayer on SiO_2 is polycrystalline with a preferred <0001> crystalline orientation, which is consistent with other published results.[16,17] The plan-view TEM image of Cu islands on Ti/SiO_2 at t_d = 10 s in Fig. 6(b) mainly shows the (110) lattice structure of fcc Cu. Although about 20% of these Cu islands show moiré fringes with periodicities of 8.7-13.5 nm, corresponding to a horizontal disorientation angle of 10-20° between the Cu [110] and Ti $[2\bar{1}\bar{1}0]$ directions, most of them have an epitaxial relationship of (111) [110] fcc-Cu || (0001) $[2\bar{1}\bar{1}0]$ hcp-Ti.[14]

The change in the crystalline orientation of nano-sized islands affects the structure of continuous thin films. The XRD patterns of 50 and 200 nm Cu thin films on SiO_2 and Ti/SiO_2 are shown in Fig. 7. Cu thin films on SiO_2 mainly show the <111> and <200> peaks, whereas those on Ti/SiO_2 only show the <111> and <222> peaks. The increased intensity and the decreased full width half maximum (FWHM) (from 0.35° for the 200 nm film on SiO_2 to 0.16° for that on Ti/SiO_2) of the Cu <111> peaks indicate the

enhanced <111> texture and the increased grain size for Cu thin films on Ti/SiO_2 compared with those on SiO_2.

C. Morphological evolution of Cu island ensembles

The island size, D, and the island number density, N_d, at deposition times of t_d = 5 and 10 s are measured from the plan-view TEM images in Fig. 5, and summarized in Table 1. Cu growth on both SiO_2 on Ti/SiO_2 shows the decrease in island number density, indicative of the island coalescence either from static growth or dynamic migration. It is noteworthy that the Cu islands on Ti/SiO_2 have a higher number density and smaller size than those on SiO_2, which can be understood from the difference in island evolution mechanisms on two substrates, as shown in the following.

We assume that Cu islands are uniformly distributed in a cell network with the unit length of $W = \left(1/N_d \right)^{1/2}$. If an island grows statically only by absorbing the incident flux to its residence unit cell, the island size, D, and inter-island distance, L, after a period of deposition can be estimated. As shown in Table 1, when t_d increases from 5 to 10 s, the diameters of Cu islands on SiO_2 and Ti/SiO_2 are estimated to increase from 3.8 to 4.1 nm, and from 2.4 to 3.2 nm, respectively. The estimated increase in island diameter by 0.3 nm for Cu islands on SiO_2 is too small compared with the inter-island distance of L = 5.0 nm at t_d = 5 s. This means that an island cannot contact and coalesce with one another if it does not migrate. In contrast, the estimated increase in island size by 0.8 nm for Cu islands on Ti/SiO_2 from t_d = 5 to 10 s is comparable with the

inter-island distance of L = 1.9 nm at t_d = 5 s. This means that island coalesce can occur even if Cu islands stay where they are formed without migration.

Therefore, the Ti underlayer changes the morphological evolution of Cu island ensembles. The lower mobility of Cu islands on Ti/SiO_2 accounts for the formation of island ensembles with a higher number density, a smaller size and inter-island distance than those on SiO_2.

IV. DISCUSSION

The 5-nm Ti underlayer changes the nano-sized Cu islands during the initial growth of Cu thin films in three aspects: the outer shape and inner structure of island individuals, and the time-dependent morphology of island ensembles. Cu islands on SiO_2 are spherical with random crystalline orientation, whereas those on Ti/SiO_2 are semi-spherical with a preferred <111> crystalline orientation. Moreover, Cu islands on Ti/SiO_2 grow with a smaller island size and inter-island distance, and a higher island number density, compared with those on SiO_2. These changes can be understood from interfacial interactions characterized by element affinity and crystallographic similarity.

The wetting angle, θ, of nano-sized Cu islands on substrates is given by the Young's equation, $\cos\theta = (\gamma_{Sub} - \gamma_{Cu/Sub})/\gamma_{Cu}$, where γ_{Cu}, γ_{Sub}, and $\gamma_{Cu/Sub}$ are the surface energies of Cu and substrates, and the interfacial energies between Cu and substrates, respectively. Cu, Ti and SiO_2 have surface energies of 1.81, 2.05, and 0.62 J/m^2, respectively.[18-20] In addition, Cu show the better affinity to Ti than to SiO_2 since various

Cu-Ti alloys are formed at temperatures as low as 800 °C. Therefore, the strong Cu-Ti interfacial interactions and the strong Cu-Cu lateral interactions dominate the formation of spherical Cu islands on SiO_2 and semi-spherical Cu islands on Ti/SiO_2, respectively. Here, $\gamma_{Cu/Ti}$ can be estimated as 0.95 ± 0.48 J/m^2 from $\theta = 50\pm20°$.

The crystalline orientation is related to the island wettability. The non-wetting Cu islands on SiO_2 have random crystalline orientation because the stability of a spherical island only depends on surface and volume factors, whichever the crystalline orientation of the island will be. However, the stability of a semi-spherical island is related to the interfacial areas and interactions. The misfit between (111) [110] fcc-Cu and (0001) [$2\bar{1}\bar{1}0$] hcp-Ti of as small as 0.04% leads to the formation of most stable <111> orientated Cu islands on the 5-nm <0001> oriented Ti underlayer on SiO_2. Although Cu islands minimize their total energy on both SiO_2 and Ti/SiO_2, the difference in the contribution of interfacial interactions leads to the formation of either random or <111> orientated crystalline Cu islands.

The changes in the evolution mechanism of Cu islands due to their mobility can be understood from interfacial interactions as well. The strong interfacial interactions between Cu and Ti/SiO_2 lead to the low mobility of wetting islands. An island stays where it is formed, and grows by absorbing incident atoms and surface diffusing adatoms. In contrast, the weak interfacial interactions between Cu and SiO_2 lead to the high mobility of non-wetting Cu islands. Therefore, not only adatoms diffuse but also islands migrate and coalesce with other islands on SiO_2 substrates, which results in the

formation of Cu islands with a larger sizes and inter-distances, and a lower number density.

It is reasonable that the decrease in melting points for small particles[21] might kinetically permit the wettability variation of nano-sized Cu islands. The crystalline orientation evolution of Cu islands on Ti/SiO_2 between t_d = 10 s and 5 s might be explained from the crystallographic reconstruction with small barriers for nano-sized islands.[22] Finally, the energy needed for structure reconstruction and migration of Cu islands might be obtained from the energy released from incorporation of adatoms and from island coalescence.[8]

Our results about the increased wettability and enhanced <111> orientation of Cu islands provide an approach for fabricating Cu-based interconnections with good adhesion and strong electromigration resistance. Cu thin films with an <111> preferred orientation have been reported to be crucial for increasing the electromigration resistance.[23] Besides, our study suggests that by controlling interfacial interactions and other factors, it is possible to fabricate islands with the desired size/distance distribution and well-defined density.

V. CONCLUSIONS

Using a 5-nm Ti underlayer, the wettability and crystalline orientation of Cu islands, as well as their size, distance and density, can be controlled from non-wetting to wetting, from random to <111> crystalline orientation, and from the adatom-diffusion-dominated

to the island-migration-dominated growth mechanism. The enhanced interfacial interactions between the Cu islands and the <0001> textured Ti underlayer, compared with those on SiO_2, lead to a change in the wettability and crystalline orientation, and adatom/island mobility. Our studies suggest that by using surface modification technologies, we should be able to fabricate nano-sized islands or continuous thin films with the desired structures and properties, because of the large contribution of interface effects on nano structures formed during the initial growth of thin films.

ACKNOWLEDGEMENTS

This work was financially supported, in part, by the New Energy and Industrial Technology Development Organization (NEDO)'s "Nanotechnology Program - Systemization of Nanotechnology Materials Program Results Project", of the Ministry of Economy, Trade, and Industry (METI), and by the Japan Society for the Promotion of Science (JSPS)’s "Grant-in-Aid for Creative Scientific Research - Establishment of Networked Knowledge System with Structured Knowledge for Future Scientific Frontier Project", of the Ministry of Education, Culture, Sports, Science and Technology (MEXT), Japan.

Table 1. Change of island number density (N_d), diameter (D), and inter-island distance (L) with deposition time (t_d). W is the cell length of the lattice structure, assuming Cu islands are uniformly distributed. Then, $W = \left(1/N_d \right)^{1/2}$, and $L = W - D$.

	t_d (s)	N_d (m^{-2})	D (nm)	L (nm)	W (nm)
On SiO_2	5	1.3×10^{16}	3.8	5.0	8.8
	10	5.4×10^{15}	7.3	6.3	13.6
	Calc.	-	4.1	4.7	-
On Ti/SiO_2	5	5.3×10^{16}	2.4	1.9	4.3
	10	1.9×10^{16}	4.9	2.4	7.3
	Calc.	-	3.2	1.1	-

Figure captions

Fig. 1. XTEM images of Cu islands on SiO_2 at deposition times of t_d = (a) 5 and (b) 10 s.

Fig. 2. XTEM images of Cu islands on Ti/SiO_2 at deposition times of t_d = (a) 5 and (b) 10 s.

Fig. 3. HRXTEM images of Cu islands on SiO_2 at deposition times of t_d = (a) 5 and (b) 10 s.

Fig. 4. HRXTEM images of Cu islands on Ti/SiO_2 at deposition times of t_d = (a) 5 and (b) 10 s.

Fig. 5. Plan-view TEM images of Cu islands on SiO_2 at deposition times of t_d = (a) 5 and (b) 10 s, and on Ti/SiO_2 at deposition times of t_d = (c) 5 and (d) 10 s, as well as the corresponding SAED patterns.

Fig. 6. Plan-view HRTEM image of (a) a 5-nm Ti underlayer on SiO_2 and (b) Cu islands on Ti/SiO_2 at t_d = 10 s, as well as the correspondign SAED pattern of Ti underlayer.

Fig. 7. XRD patterns of 50- and 200-nm Cu thin films on (a) SiO_2 and (b) Ti/SiO_2, and (c) illustration of Cu powder pattern indicating peak intensity and position [Ref. JCPDS 4-0836]. Two peaks at 34.6° and 69.2° originate from Si substrates.

References

[1]V. Musolino, A. Dal Corso, and A. Selloni, Phys. Rev. Lett. **83**, 2761 (1999).

[2]M. Hu, S. Noda, and H. Komiyama, Surf. Sci. **513**, 530 (2002).

[3]D. Fuks, S. Dorfman, Y. F. Zhukovskii, E. A. Kotomin, and A. M. Stoneham, Surf. Sci. **499**, 24 (2002).

[4]K. Kizuka and N. Tanaka, Phys. Rev. B **56**, R10079 (1997).

[5]S. Bajt, D. G. Steams, and P. A. Kearney, J. Appl. Phys. **90**, 1017 (2001).

[6]M. Jose-Yacaman, M. Marin-Almazo, and J. A. Ascencio, J. Mol. Catal. A **173**, 61 (2001).

[7]M. Hu, S. Noda, and H. Komiyama, J. Appl. Phys. **93**, 9336 (2003).

[8]H. Shirakawa and H. Komiyama, J. Nanoparticle Research **1**, 17 (1999).

[9]V. Dureuil, C. Ricolleau, M. Gandais, C. Grigis, J. P. Lacharme, and A. Naudon, J. Crystal Growth **233**, 737 (2001).

[10]M. Hu, S. Noda, Y. Tsuji, T. Okubo, Y. Yamaguchi, and H. Komiyama, J. Vac. Sci. Technol. A **20**, 589 (2002).

[11]J. M. Zuo and B. Q. Li, Phys. Rev. Lett. **88**, 2555021 (2002).

[12]P. B. Abel, A. L. Korenyi-Both, F. S. Honecy, and S. V. Pepper, J. Mater. Research **9**, 617 (1994).

[13]S. W. Russell, S. A. Rafalski, R. L. Spreitzer, J. Li, M. Moinpour, F. Moghadam, and T. L. Alford, Thin Solid Films **262**, 154 (1995).

[14]G. Dehm, C. Scheu, M. Ruhle, and R. Raj, Acta Mater. **46**, 759 (1998).

[15]Y. K. Ko, J. H. Jang, S. Lee, H. J. Yang, L. W. H., P. J. Reucroft, and J. G. Lee, J. Mater. Sci. **38**, 217 (2003).

[16]T. Ohwaki, T. Yoshida, S. Hashimoto, H. Hosokawa, Y. Mitsushima, and Y. Taga, Jpn. J. Appl. Phys. **36**, L154 (1997).

[17]D. N. Dunn, R. Hull, F. M. Ross, and R. M. Tromp, J. Appl. Phys. **89**, 2635 (2001).

[18]W. R. Tyson and W. A. Miller, Surf. Sci. **62**, 267 (1977).

[19]L. Z. Mezey and J. Giber, Jpn. J. Appl. Phys. **21**, 1569 (1982).

[20]S. H. Overbury, P. A. Bertrand, and G. A. Somorjai, Chem. Rev. **75**, 547 (1975).

[21]J.-P. Borel, Surf. Sci. **106**, 1 (1981).

[22]M. J. Yacaman, J. A. Ascencio, H. B. Liu, and J. Gardea-Torresdey, J. Vac. Sci. Technol. B **19**, 1091 (2001).

[23]C. S. Ryu, K. W. Kwon, A. L. S. Loke, H. B. Lee, T. Nogami, V. M. Dubin, R. A. Kavari, G. W. Ray, and S. S. Wong, IEEE Trans. Electron Devices **46**, 1113 (1999).

Fig. 1

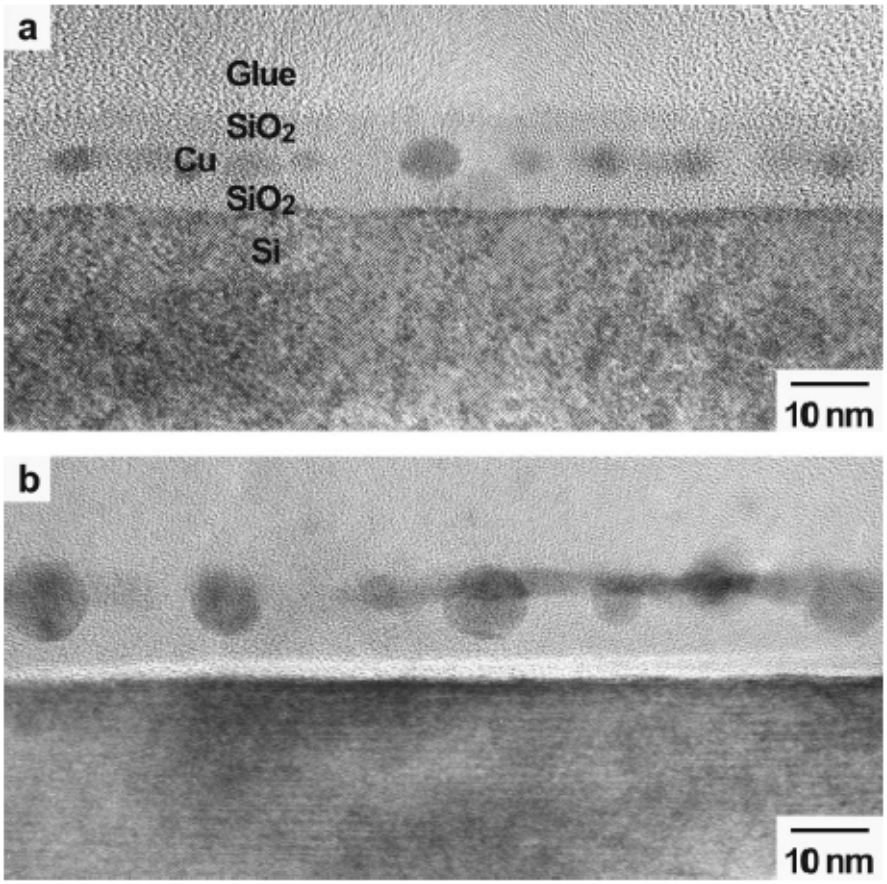

Fig. 2

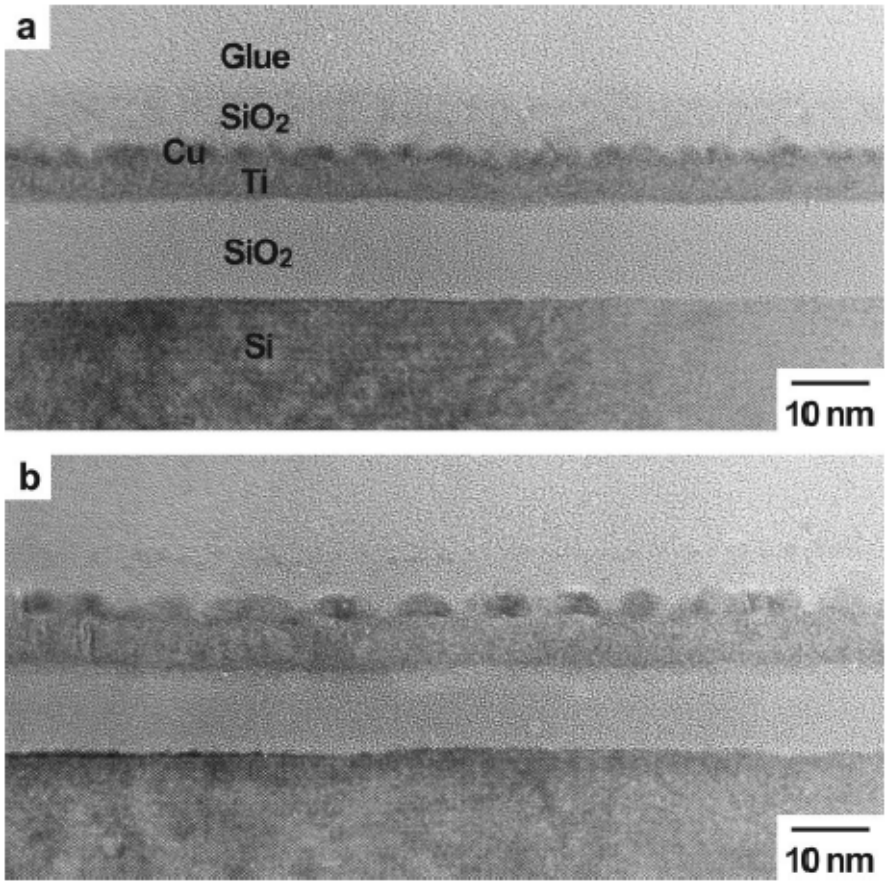

Fig. 3

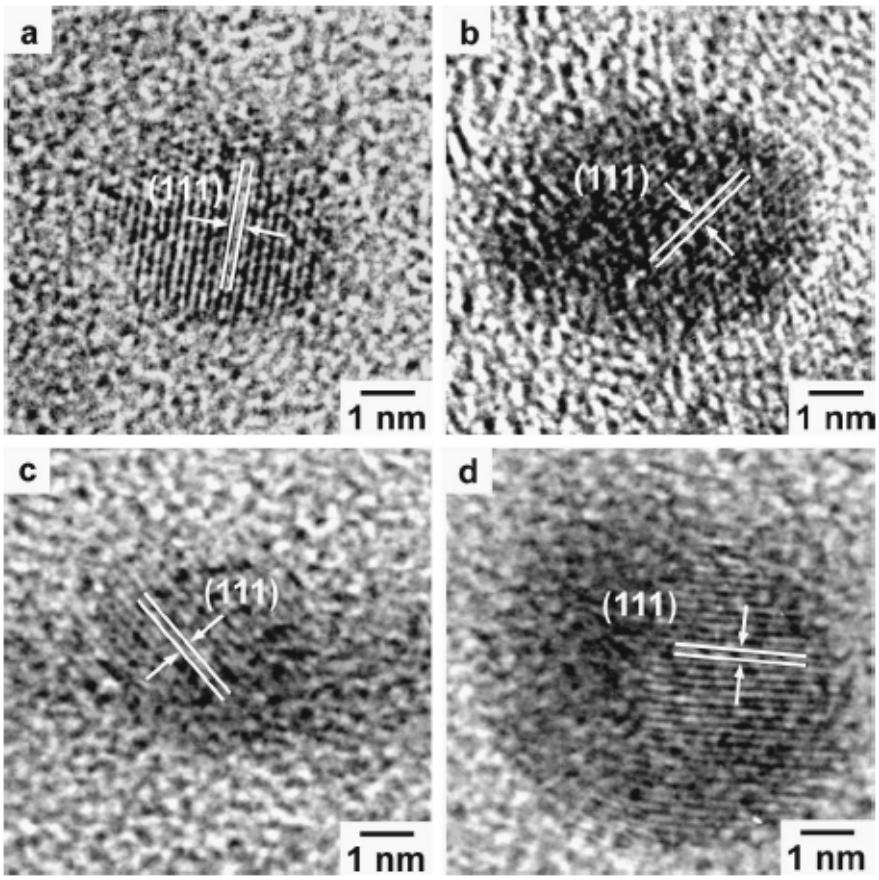

Fig. 4

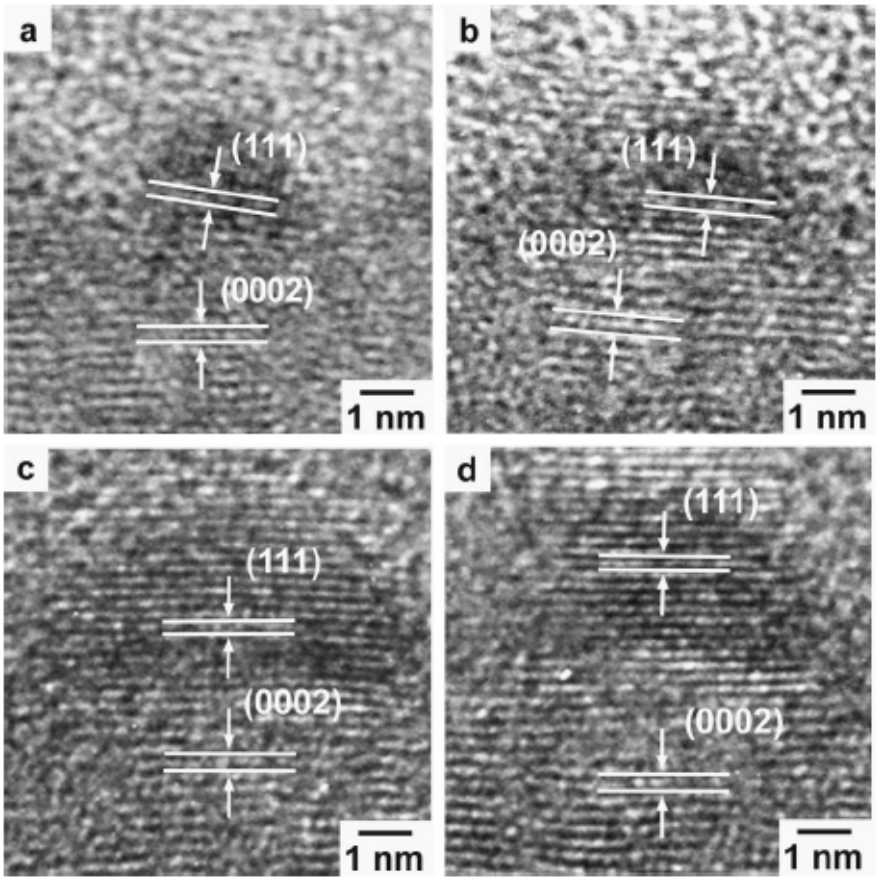

Fig. 5

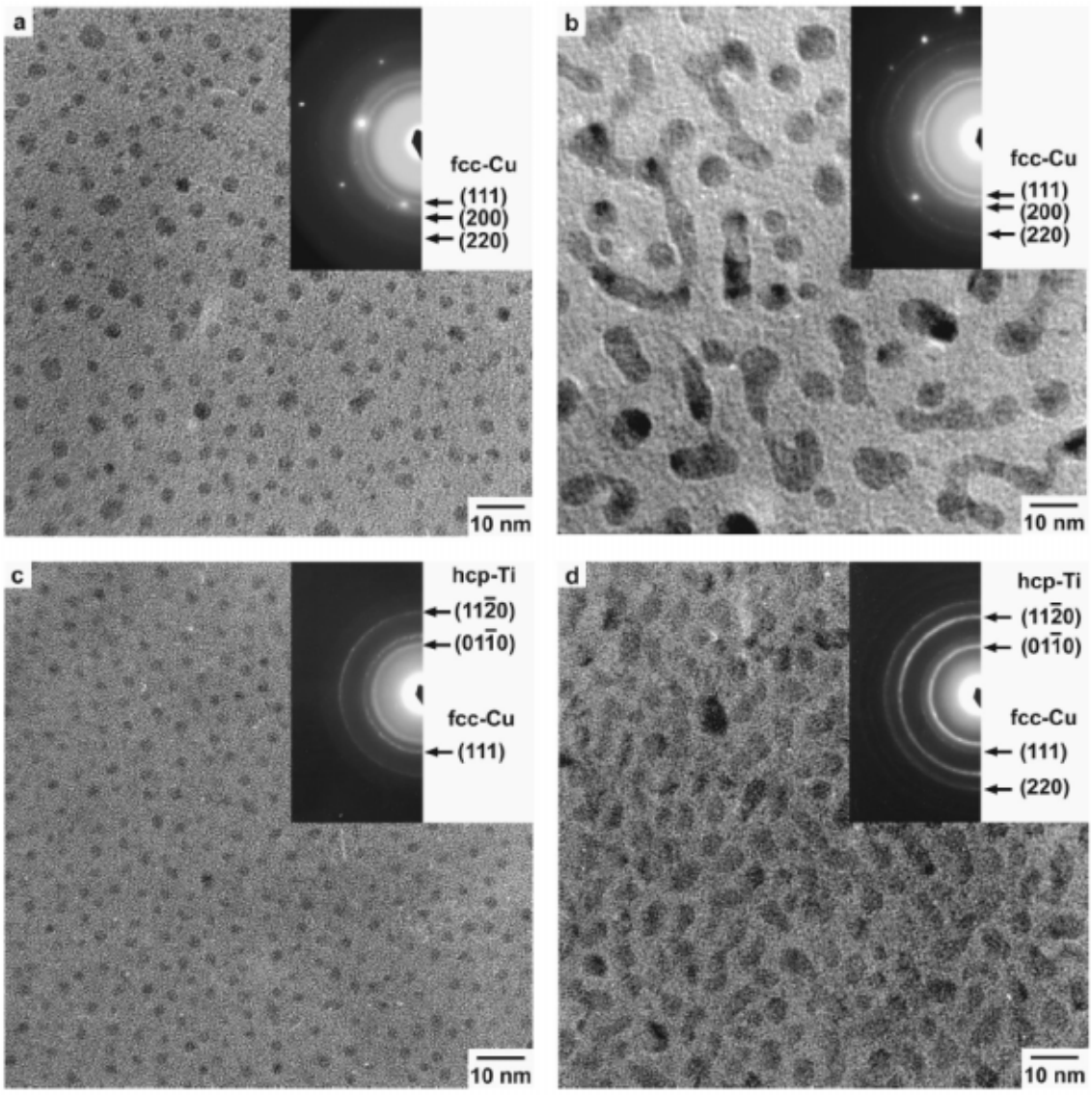
a
fcc-Cu
(111)
(200)
(220)
10 nm
b
fcc-Cu
(111)
(200)
(220)
10 nm
c
hcp-Ti
(11$\bar{2}$0)
(01$\bar{1}$0)
fcc-Cu
(111)
10 nm
d
hcp-Ti
(11$\bar{2}$0)
(01$\bar{1}$0)
fcc-Cu
(111)
(220)
10 nm

Fig. 6

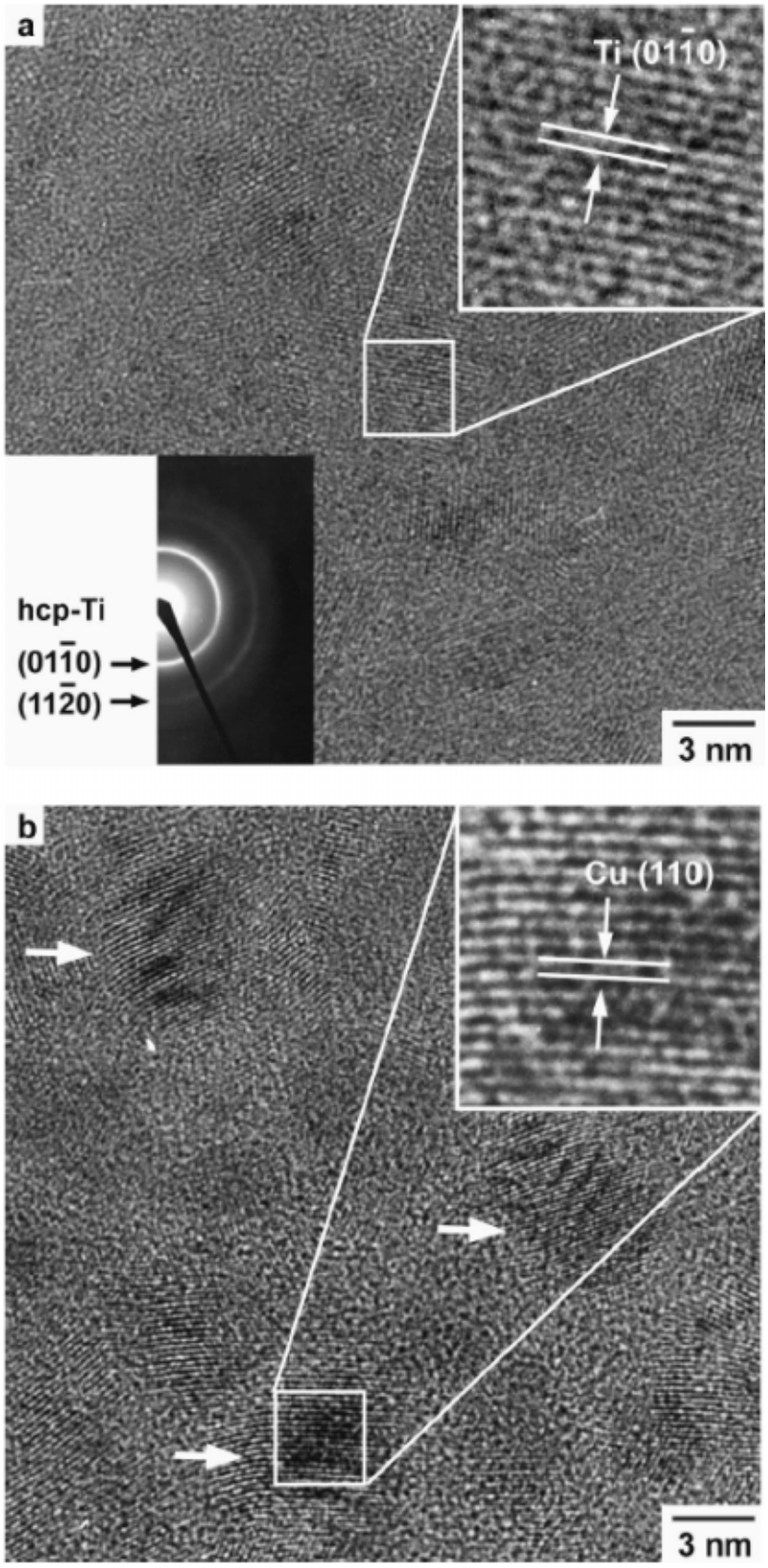

Fig. 7

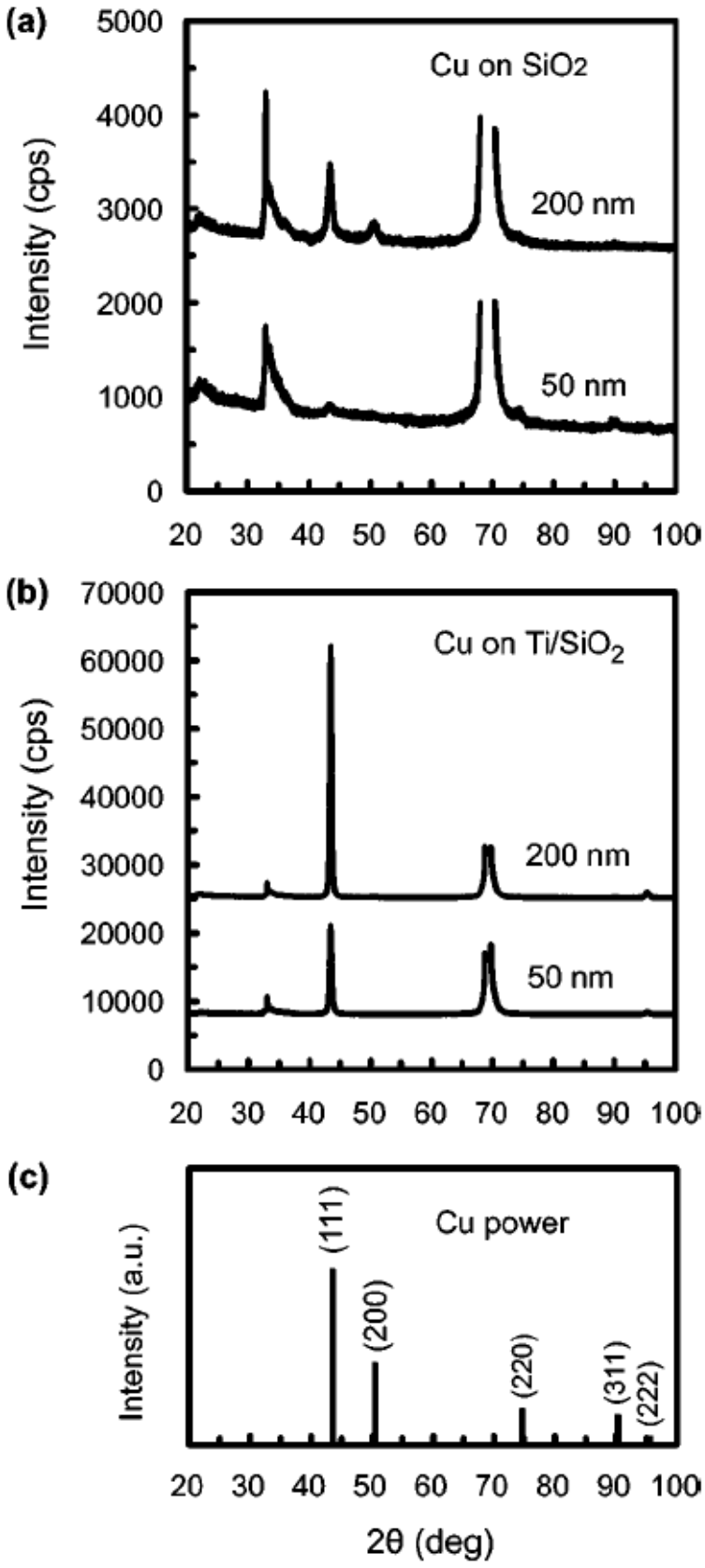
(a)
Cu on SiO2
200 nm
50 nm
Intensity (cps)
5000
4000
3000
2000
1000
0
20 30 40 50 60 70 80 90 100
(b)
Cu on Ti/SiO2
200 nm
50 nm
Intensity (cps)
70000
60000
50000
40000
30000
20000
10000
0
20 30 40 50 60 70 80 90 100
(c)
Cu power
(111)
(200)
(220)
(311)
(222)
Intensity (a.u.)
20 30 40 50 60 70 80 90 100
2θ (deg)